Solitons in combined linear and nonlinear lattice potentials

Hidetsugu Sakaguchi[1] and Boris A. Malomed[2]
[1]Department of Applied Science for Electronics and Materials,
Interdisciplinary Graduate School of Engineering Sciences,
Kyushu University, Kasuga, Fukuoka 816-8580, Japan
[2]Department of Physical Electronics,
School of Electrical Engineering, Faculty of Engineering,
Tel Aviv University, Tel Aviv 69978, Israel

January 5, 2010

abstract

We study ordinary solitons and gap solitons (GSs) in the framework of the one-dimensional Gross-Pitaevskii equation (GPE) with a combination of linear and nonlinear lattice potentials. The main points of the analysis are effects of (in)commensurability between the lattices, development of analytical methods, *viz.*, the variational approximation (VA) for narrow ordinary solitons, and various forms of the averaging method for broad solitons of both types, and also the study of mobility of the solitons. Under the direct commensurability (equal periods of the lattices, $L_{\mathrm{lin}} = L_{\mathrm{nonlin}}$), the family of ordinary solitons is similar to its counterpart in the GPE without external potentials. In the case of the subharmonic commensurability, with $L_{\mathrm{lin}} = (1/2)L_{\mathrm{nonlin}}$, or incommensurability, there is an existence threshold for the ordinary solitons, and the scaling relation between their amplitude and width is different from that in the absence of the potentials. GS families demonstrate a bistability, unless the direct commensurability takes place. Specific scaling relations are found for them too. Ordinary solitons can be readily set in motion by kicking. GSs are mobile too, featuring inelastic collisions. The analytical approximations are shown to be quite accurate, predicting correct scaling relations for the soliton families in different cases. The stability of the ordinary solitons is fully determined by the VK (Vakhitov-Kolokolov) criterion, i.e., a negative slope in the dependence between the solitons's chemical potential μ and norm N. The stability of GS families obeys an inverted ("anti-VK") criterion, $d\mu/dN > 0$, which is explained by the approximation based on the averaging method. The present system provides for a unique possibility to check the anti-VK criterion, as $\mu(N)$ dependences for GSs feature turning points, except for the case of the direct commensurability.

1   Introduction

It is well known that periodic potentials, induced by optical lattices (OLs), provide for a versatile tool for controlling dynamics of Bose-Einstein condensates (BECs). This tool is especially efficient for the creation and stabilization of solitons – both ordinary ones and gap solitons (GSs), which are supported by the interplay of the OL potential and self-repulsive nonlinearity. Many results obtained in theoretical and experimental studies of this topic were summarized in reviews focused on one-dimensional (1D) [1] and multidimensional [2] matter-wave dynamics. Earlier, a similar model was introduced in optics for the description of spatial solitons in nonlinear waveguides with a periodic transverse modulation of the refractive index [3]. In the experiment, lattices controlling the transmission of optical beams were implemented in the form of photoinduced gratings in photorefractive crystals, which made it possible to create various species of 1D and 2D spatial solitons [4]. Gratings were also created as permanent structures written by femtosecond laser beams in silica [5]. Recently, this topic was reviewed in Ref. [6]; a closely related topic is the study of discrete solitons in optics, which was a subject of another comprehensive review in Ref. [7].

A different possibility, which has drawn much attention in studies of BEC (thus far, primarily at the theoretical level), is the use of a spatially profiled effective nonlinearity, that may be implemented by means of properly designed configurations of external fields via the Feshbach-resonance effect. In terms of the condensed-matter theory, the nonuniform nonlinearity coefficient induces an effective *pseudopotential* [8, 9], that can be used to control the dynamics of localized modes. Various problems of this sort were considered in 1D settings, with periodic pseudopotentials in the form of nonlinear lattices (NLs) [10, 11, 12], as well as with spatial modulations of the nonlinearity coefficient represented by one [13] or two [9] delta-functions (actually, the model with the self-attractive nonlinearity concentrated at a single delta-function was introduced long ago as a model for tunneling of interacting particles through a junction [14]). In particular, the configuration with two delta-functions makes it possible to study spontaneous symmetry breaking of matter waves trapped by a symmetric double-well pseudopotential [9]. Specially chosen profiles of the nonlinearity coefficient may also be employed to design a pulse-generating atomic-wave laser [15], as well as traps and barriers for such pulses [16]. The analysis of 1D matter-wave solitons in NLs was further extended for two-component models [17, 18], and for some spatiotemporal patterns of the nonlinearity modulation [19]. Certain results for solitons supported by 2D nonlinear pseudopotentials were reported too, although the stabilization of 2D solitons in this setting is a tricky problem [20].

In addition to the BEC, a periodic modulation of the nonlinearity is possible in optics, where it was analyzed in terms of temporal [21] and spatial [22, 23] solitons. A discussion of practical possibilities to create NLs in optical media in the "pure form" (without affecting the linear properties, i.e., the refractive index) can be found in recent paper [18]. An experimental observation of NL-supported optical solitons (in the form of surface solitons at an interface between lattices) was reported in Ref. [24].

A natural generalization of the study of NL pseudopotentials is to consider atomic and optical media equipped with a combination of nonlinear and linear lattices, in 1D [25, 26, 12] and 2D [27] settings. In the experiment, this may be implemented by applying the above-mentioned techniques simultaneously – for instance, combining the OL, which induces the linear periodic potential in the BEC, and the patterned magnetic field, which gives rise to the nonlinear pseudopotential via the Feshbach resonance. Actually, photonic-crystal fibers, where various species of spatial solitons

have been predicted [28], also belong to this type of media. Under special conditions, the combined models admit analytical solutions, see Ref. [12] and references therein. In particular, exact solutions were elaborated in detail for the lattices of the Kronig-Penney (piecewise-constant) type [23].

The objective of this work is to investigate the existence, stability, and mobility of ordinary 1D solitons and their GS counterparts in the combined NL-OL model, with emphasis on effects of the *commensurability* (spatial resonance) between the nonlinear and linear lattices. In the general case, the solitons are found in a numerical form. For narrow ordinary solitons (those whose chemical potential, μ, falls into the semi-infinite gap of the linearized version of the model), we also develop a variational approximation (VA). For broad solitons, both ordinary ones and GSs with μ belonging to the first finite bandgap, we elaborate analytical approximations based on different versions of the averaging technique.

The stability of the solitons is investigated below by means of systematic simulations of their perturbed evolution. We conclude that the well-known VK (Vakhitov-Kolokolov) criterion [29] completely determines the actual stability of the ordinary solitons (the criterion states that a necessary stability condition is a negative slope in the dependence of the solitons' chemical potential, μ, on their norm, N, i.e., $d\mu/dN < 0$). For the GS families, our analysis leads to a different conclusion: their stability fully obeys an "anti-VK" criterion, *viz.*, $d\mu/dN > 0$. As a matter of fact, all stable GS families in previously studied models had only the positive slope of $\mu(N)$, thus satisfying the latter criterion automatically. However, the present model offers a rather unique chance to test it in a nontrivial situation, when $\mu(N)$ curves for the GSs may have portions with both positive and negative slope, separated by turning points. Using the averaging method, we also produce a justification for the anti-VK criterion, which is relevant, at least, for subfamilies of broad GSs.

The rest of the paper is organized as follows. The model is formulated in the next section, which also reports basic numerical results. In the case of the direct commensurability between the nonlinear and linear lattices (for those with equal periods, $L_{\mathrm{lin}} = L_{\mathrm{nonlin}}$), it is concluded that ordinary solitons are similar to soliton solutions of the nonlinear Schrödinger equation (NLSE) in the free space (without an external potential), in the sense that there is no threshold for their existence, the entire soliton family is stable, and the amplitude and width of the soliton, A and W, obey the usual scaling relation, $A \propto 1/W$. On the contrary to that, there is an existence threshold for ordinary solitons in the case of the incommensurability, or if the commensurability (spatial resonance) between the lattices is *subharmonic*, with $L_{\mathrm{lin}} = L_{\mathrm{nonlin}}/2$. In those cases, the scaling relation between the amplitude and width is different too – featuring, in particular, $A \propto 1/W^2$ for the subharmonic resonance. The same commensurability-depending change in the scaling is observed in GS families, which also demonstrate a bistability in cases different from the direct commensurability.

Analytical results, which may explain a considerable part of the numerical findings, are collected in Section III. First, we develop the VA for narrow ordinary solitons, and then the averaging method is reported, in different forms for different cases. It is demonstrated that both the VA and averaging produce results which are in good agreement with numerical observations, in relevant regions of the parameter space. In particular, as briefly mentioned above, the averaging lends an explanation to the "anti-VK" stability criterion for GSs. In the case of $L_{\mathrm{lin}} = L_{\mathrm{nonlin}}/2$, an average equation for the envelope amplitude includes a quintic nonlinear term, rather than the cubic one, which accounts for the above-mentioned change in the scaling relation between A and W. The paper is concluded by Section IV.

3

2 Numerical results

2.1 The model

The model combining the linear OL potential and nonlinear NL pseudopotential is based on the known effectively one-dimensional Gross-Pitaevskii equation for the mean-field wave function, $\phi(x,t)$ [23, 25, 26, 12]. In the scaled form, the equation is

$$i\phi_t = -(1/2)\phi_{xx} - \left[\epsilon\cos(2\pi x) + g\cos(\pi qx)\,|\phi|^2\right]\phi, \tag{1}$$

where ϵ is the strength of the linear OL, and $g = \pm 1$ is fixed by the normalization. The NL wavenumber is q, the above-mentioned periods of the linear and nonlinear lattices being $L_{\mathrm{lin}} \equiv 1$ and $L_{\mathrm{nonlin}} = 2/q$. For $q = 0$ and $g = -1$, Eq. (1) amounts to the NLSE with the OL potential and constant coefficient in front of the self-defocusing cubic term. As is well known, this equation supports families of stable GS solutions [1, 30]. On the other hand, in the absence of the OL, $\epsilon = 0$, the NL supports ordinary solitons, but not GSs [10, 11, 12].

Stationary solutions with chemical potential μ are looked for in the form of $\phi(x,t) = u(x)\exp(-i\mu t)$, where $u(x)$ is a real function. The substitution of this expression into Eq. (1) yields an ordinary differential equation,

$$\mu u = -(1/2)\,u'' - \left[\epsilon\cos(2\pi x) + g\cos(\pi qx)u^2\right]u, \tag{2}$$

which can be derived from the corresponding Lagrangian,

$$2L = \int_{-\infty}^{+\infty}\left[\mu u^2 - (1/2)\left(u'\right)^2 + \epsilon\cos\left(2\pi x\right)\,u^2 + (g/2)\cos\left(\pi qx\right)\,u^4\right]dx. \tag{3}$$

We have constructed numerical solutions for localized stationary modes by means of the shooting method applied to Eq. (2). The stability of the so found solutions against small perturbations was tested through direct simulations of Eq. (1). The results were also compared to predictions of the VK criterion for the ordinary solitons, and to the above-mentioned "anti-VK" criterion for GSs. Numerical results reported below are obtained for the OL strength $\epsilon = 5$, which adequately represents the generic situation, for the ordinary solitons and GSs alike.

Figures 1(a) and (b) display, respectively, examples of ordinary solitons (for $g = +1$, $q = 1$) and GSs (for $g = -1$, $q = 1$) with equal amplitudes. The choice of $q = 1$ corresponds to the above-mentioned case of the subharmonic resonance between the OL and NL, $L_{\mathrm{lin}} = (1/2)L_{\mathrm{nonlin}}$. In this case, stable ordinary solitons and GSs coexist for either sign of g. If, for instance, $g = +1$, ordinary solitons are located around even sites of the NL, $x = 2n$ (with integer n), while GSs may be centered at odd sites, $x = 2n + 1$.

2.2 Ordinary solitons

Figure 2(a) represents a family of the ordinary solitons, by means of the relation between their norm, $N = \int_{-\infty}^{+\infty} u^2(x)dx$, and chemical potential μ, at three characteristic values of the NL's wavenumber, $q = 1$, $\sqrt{5}-1$, and 2, for $g = +1$. These values are chosen because $q = 2$ corresponds to the direct commensurability between the linear and nonlinear lattices ($L_{\mathrm{lin}} = L_{\mathrm{nonlin}}$), $q = 1$ represents, as said above, the subharmonic commensurability $[L_{\mathrm{lin}} = (1/2)L_{\mathrm{nonlin}}]$, and $q = \sqrt{5} - 1$ corresponds to incommensurate lattices. All values of μ for the ordinary solitons fall into the semi-infinite gap of the spectrum induced by the OL potential in the linearized version of Eq. (1).
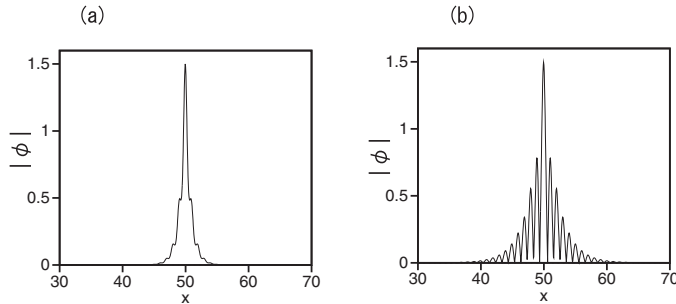
4

Figure 1: Typical examples of a stable broad ordinary soliton (a) and stable gap soliton (b), at $g = +1$ and -1, respectively, in the case of the nonlinear lattice with period $L_{\mathrm{nonlin}} = 2$ (i.e., $q = 1$). The amplitudes of both solitons are $A = 1.5$. The chemical potential and norm are, respectively, $\mu = -1.198$ and $N = 1.628$ for the ordinary soliton, and $\mu = 2.629$ and $N = 2.176$ for the gap soliton.

At $q = 2$, direct simulations demonstrate that the entire soliton family is stable, precisely as suggested by the VK criterion, $d\mu/dN < 0$, see Fig. 2(a). For $q = 1$ and $q = \sqrt{5} - 1$, the results are different, featuring non-monotonous relations $\mu(N)$. Accordingly (again in the agreement with the prediction of the VK criterion), narrow solitons with larger amplitudes, which correspond to the branches of $\mu(N)$ with $d\mu/dN < 0$ in Fig. 2(a), are stable, while their loosely bound (broad) counterparts, corresponding to the branches with $d\mu/dN > 0$, are unstable. Another difference from the case of the direct commensurability is that there is a minimum value of the norm, $N_{\min}$ (the threshold), which is necessary for the existence of the ordinary solitons at $q = 1$ and $\sqrt{5} - 1$, while there is no threshold at $q = 2$.

In fact, the situation in the case of $q = 1$ and $\sqrt{5} - 1$ – the existence of the threshold value, $N_{\min}$, which separates stable and unstable branches of the ordinary-soliton solutions – is qualitatively similar to what is known in the model with the NL but no linear potential [10]. On the other hand, the situation in the case of $q = 2$ – the absence of $N_{\min}$ and the existence of the single branch of the soliton solutions, which is entirely stable – resembles well-known properties of soliton solutions of the NLSE without any lattice, linear or nonlinear.

The evolution of those ordinary solitons which are unstable is illustrated in Fig. 3 for $q = 1$ and $g = +1$. It is observed that the unstable soliton, with initial amplitude $A = 0.9$, rearranges itself into a narrower persistent breather, with time-average amplitude $A_{\mathrm{br}} \approx 1.1$, while the norm is kept constant. The transformation of the unstable ordinary solitons into stable breathers is also similar to what was reported in the model without the OL [10].

Properties of the ordinary solitons in the same three families, with $q = 1, \sqrt{5} - 1$ and 2 (and $g = +1$), are further illustrated in Fig. 2(b) through relations between the soliton's amplitude, A, and its width, W, which we define by

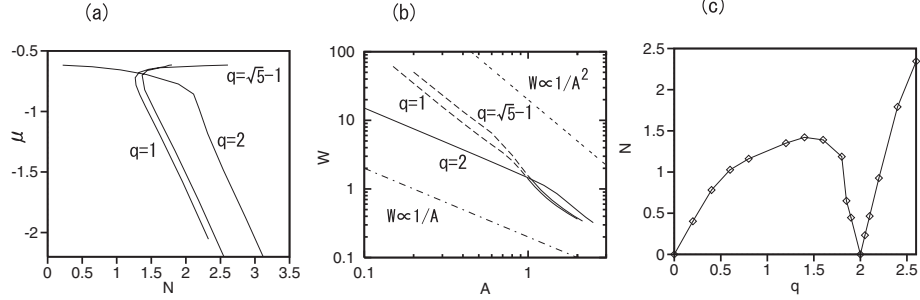$$W^2 = N^{-1} \int_{-\infty}^{+\infty} |\phi(x)|^2 \, (x - L/2)^2 \, dx \tag{4}$$

5

Figure 2: (a) Chemical potential μ versus norm N for families of ordinary solitons at different values of q and $g = +1$. Portions of the curves with $d\mu/dN < 0$ and $d\mu/dN > 0$ represent, respectively, stable and unstable (sub)families, in agreement with the VK criterion. (b) The log-log plot of amplitude A versus width W [the latter is defined as per Eq. (4)]. Bold dashed lines correspond to unstable branches of the soliton families, for $q = 1$ and $\sqrt{5}-1$. Thin dashed reference lines designate scalings which different families obey at small values of A, namely, $W \propto 1/A$ and $W \propto 1/A^2$. (c) The stability boundary for the ordinary solitons, which is defined, as per the VK criterion, by condition $dN/d\mu = 0$. As predicted by the criterion and verified in direct simulations, the solitons are stable above the boundary.
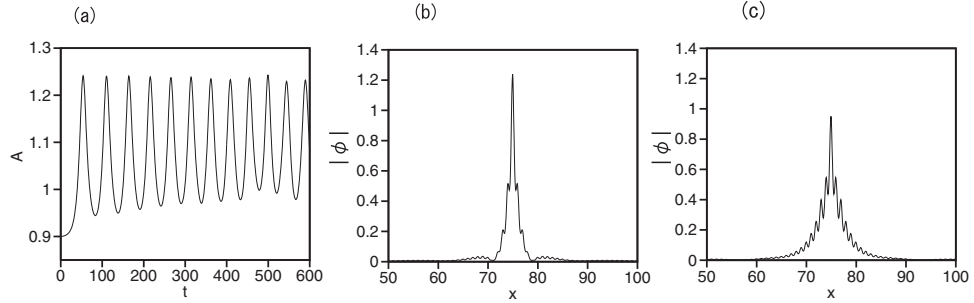

Figure 3: An example of the spontaneous rearrangement of an unstable ordinary soliton, with amplitude $A = 0.9$ and norm $N = 1.32$, into a robust breather, at $q = 1$ and $g = +1$. (a) The evolution of the soliton's amplitude. (b) The field profile, $|\phi(x,t)|$, at $t = 110$. (c) The profile at $t = 140$. Panels (b) and (c) display the shape of the breather at points where its width is close, respectively, to the minimum and maximum values.

6

($x = L/2$ is the central point of the integration domain). At $q = 2$, relation $W(A)$ features scaling $W \propto 1/A$ for relatively small values of A. This is the same scaling as featured by exact soliton solutions of the NLSE in the free space, which is in line with the above observation that the soliton family at $q = 2$ is similar to that in the NLSE without any lattice. However, the scaling is different in the other families, featuring $W(A) \propto 1/A^2$ for $q = 1$, and $W(A) \propto 1/A^{1.8}$ for $q = \sqrt{5} - 1$. The two latter scaling relations imply that the width of the respective solitons is essentially larger than in their free-space counterparts, therefore we call them broad solitons.

Figure 2(c) summarizes the results by means of the stability boundary for the ordinary solitons in the plane of (q, N). The boundary is identified as a VK-critical curve, along which $d\mu/dN$ vanishes, the stability area (with $d\mu/dN < 0$) being located above the curve. Systematic simulations performed in regions below and above the boundary have confirmed that the solitons in these regions are, respectively, unstable and stable (unstable solitons transform themselves into breathers, as shown in Fig. 3). The stability area reaches the limit of $N = 0$ (very broad solitons with a vanishingly small amplitude) in the form of the cusps in Fig. 2(c) at $q = 0$ and $q = 2$. Recall that $q = 0$ with $g = +1$ corresponds to the constant coefficient of the self-attractive nonlinearity in Eq. (1), while $q = 2$ corresponds to the direct commensurability between the linear and nonlinear lattices.

2.3   Static gap solitons

In this work, the consideration of GS families was confined to the first finite bandgap induced by the OL potential, in terms of the linearized version of Eq. (1). The $N(\mu)$ and $W(A)$ curves for these families are displayed in Figs. 4(a) and (b), for the same three cases as above, $viz.$, $q = 1, \sqrt{5} - 1$ and 2, fixing $g = -1$ [width W is again defined as per Eq. (7)]. The VK criterion does not apply to GSs. Nevertheless, the results strongly suggest that the stability of all GS families follows an "$anti$-VK" condition, $d\mu/dN > 0$. For subfamilies of broad GSs, this condition is derived below from an effective envelope equation for broad GSs which amounts to an "inverted" NLSE, with the self-repulsive nonlinear term and negative effective mass, see Eqs. (15). In that approximation, GSs reduce to ordinary solitons if the wave function is subjected to the complex conjugation, which implies the inversion of the sign of μ, and of $d\mu/dN$ as well.

In accordance with what is said above, the entire GS family for $q = 2$, which satisfies the "anti-VK" condition everywhere in Fig. 4(a), is found to be completely stable in direct simulations. On the other hand, the $\mu(N)$ curves for $q = 1$ and $q = \sqrt{5} - 1$ feature two folds, and direct simulations corroborate the instability of portions of the GS families with $d\mu/dN < 0$. To the best of our knowledge, the present model produces the first example of $\mu(N)$ characteristics for GSs with turning points, which makes the anti-VK criterion amenable to the actual verification. In the standard model with the constant nonlinearity coefficient [32, 1], as well as in its version with the quasiperiodic OL potential [33], the monotonous character of the curves does not allow the verification of the criterion.

The stability diagram in the plane of (q, N), as predicted by the "anti-VK" criterion, is displayed in Fig. 4(c). It includes two critical curves with $dN/d\mu = 0$. As suggested by Fig. 4(b), and completely confirmed by systematic simulations, in the regions above the top curve and below the bottom one there is a single solution, which is stable. Between the curves, there are three solutions, two of which are stable, i.e., this is a *bistability* region. The critical curves feature cusps near $q = 0$ and $q = 2$,
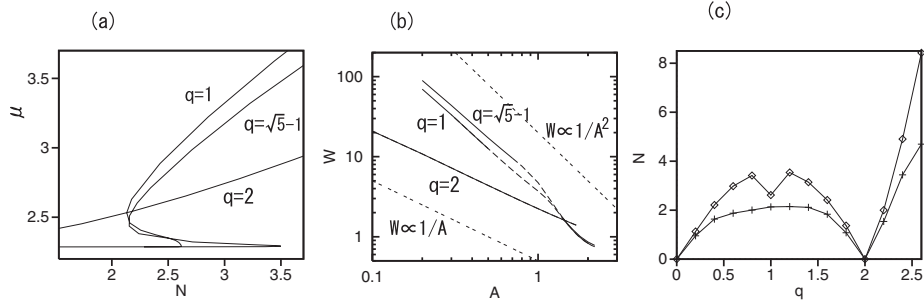
7

Figure 4: (a) The relation between norm N and chemical potential μ of gap solitons for $q = 1, \sqrt{5} - 1$, and 2, for $g = -1$. Portions of the curves with $d\mu/dN > 0$ and $d\mu/dN < 0$ represent stable and unstable (sub)families, respectively, obeying the "anti-VK" criterion (see the text). (b) The log-log plot of amplitude A versus width W, for the gap solitons. Bold dashed portions of the curves correspond to unstable solutions, with $d\mu/dN < 0$. Thin dashed reference lines designate scalings $W \propto 1/A$ and $W \propto 1/A^2$. (c) Critical lines $dN/d\mu = 0$ in the plane of (q, N). There is a single stable gap soliton above the upper line and beneath the lower one, and three solutions – two stable and one unstable – in the bistability region between the two lines.

similar to the situation displayed in Fig. 2(c).

From Fig. 4(b) we conclude that the scaling relations between the GS's width and amplitude for broad solitons (with small values of A) take the following form: For $q = 2$, $W \sim 1/A$; for $q = \sqrt{5} - 1$, $W \propto 1/A^{1.85}$; and for $q = 1$, $W \propto 1/A^2$, i.e., almost exactly the same as their counterparts for the ordinary solitons, see above. All portions of the GS families obeying these scaling relations are stable. On the other hand, the simulations demonstrate that unstable GSs (those with $d\mu/dN < 0$) are not transformed into breathers, unlike unstable ordinary solitons, but rather suffer a gradual decay into quasi-linear waves (not shown here).

3 Analytical methods

3.1 The variational approximation for ordinary solitons

Narrow stationary solitons of the ordinary type (corresponding to $g = +1$) can be naturally approximated by means of the VA, using the simplest Gaussian ansatz [3],

$$u(x) = A \exp\left[-x^2/\left(2W^2\right)\right],\tag{5}$$

with norm $N = \sqrt{\pi} A^2 W$. The substitution of ansatz (5) in Lagrangian (3) yields the effective Lagrangian, written in terms of the norm, instead of amplitude A:

$$2L_{\text{eff}} = \mu N - \frac{N}{4W^2} + \epsilon N e^{-\pi^2 W^2} + \frac{N^2}{2\sqrt{2}W} e^{-\pi^2 q^2 W^2/8}.\tag{6}$$
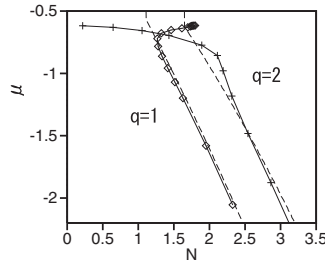
8

Figure 5: Comparison of the variational (dashed lined) and numerically found (chains of symbols) curves $\mu(N)$ for ordinary solitons ($g = +1$).

Variational equations following from Eq. (6), $\partial L_{\text{eff}}/\partial W = 0$ and $\partial L_{\text{eff}}/\partial N = 0$, take the form of

$$4\pi^2 \epsilon W^4 e^{-\pi^2 W^2} + \left(1/\sqrt{2\pi}\right)\left(1 + \pi^2 k^2 W^2\right) N W e^{-(\pi q W)^2/8} = 1, \qquad (7)$$

$$\left(4W^2\right)^{-1} - \epsilon e^{-(\pi W)^2} - \left(1/\sqrt{2\pi}\right)(N/W) e^{-(\pi q W)^2/8} = \mu. \qquad (8)$$

Figure 5 compares the $\mu(N)$ curves produced by Eqs. (7) and (8) to their numerically found counterparts, for the NL wavenumbers $q = 1$ and 2. It is seen that the VA provides for a good approximation for narrow solitons with values of μ which are not too close to the edge of the semi-infinite gap. Portions of the curves corresponding to broad solitons, which are located near the gap's edge, are not captured by the VA, as the actual shape of these solitons is different from the Gaussian, see, e.g., Fig. 1(a).

3.2   The averaging method

3.2.1   Ordinary solitons

The approximation based on averaging can be applied to broad solitons, which have a small amplitude and large norm. In the case of the ordinary solitons ($g = +1$), this is the situation opposite to that (narrow localized modes) for which the VA was presented in the previous section. To develop the averaging approach for ordinary solitons, we adopt the ansatz

$$\phi(x,t) = \Phi(x,t)\left[1 + 2\alpha \cos(2\pi x)\right], \qquad (9)$$

where the slowly varying amplitude function, Φ, multiplies the simplest approximation for the Bloch wave function which may be used near the edge of the semi-infinite gap, with $\alpha = \left(\sqrt{\pi^4 + \epsilon^2/2} - \pi^2\right)/\epsilon$ (this approximation is obtained by dint of the analysis presented in Ref. [30]). The substitution of ansatz (9) into Eq. (1) and averaging, also performed along the lines of Ref. [30], lead to the asymptotic NLSE for the slowly varying envelope function,

$$i\frac{\partial \Phi}{\partial t} = -\frac{1}{2m_{\text{eff}}^{(\text{ord})}}\frac{\partial^2 \Phi}{\partial x^2} + g_{\text{eff}}^{(\text{ord})}|\Phi|^2\Phi, \qquad (10)$$
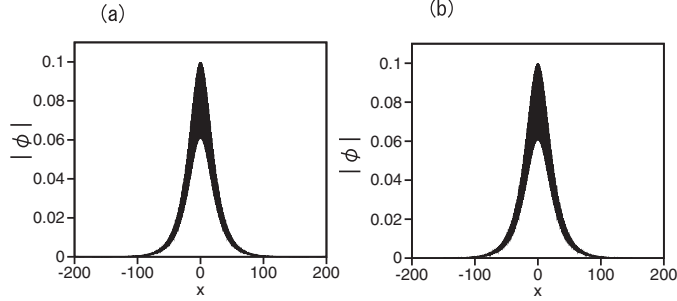
9

Figure 6: (a) The numerical obtained profile of an ordinary soliton with amplitude $A = 0.1$ for $g = +1$ and $q = 2$. (b) The profile predicted for the same soliton by means of the averaging method, see Eqs. (9), (13), (11), and (12).

where the calculations yield the following coefficients:

$$m_{\text{eff}}^{(\text{ord})} = \frac{2\pi^4 + \epsilon^2 + \pi^2\sqrt{4\pi^4 + 2\epsilon^2}}{10\pi^4 + \epsilon^2 - 3\pi^2\sqrt{4\pi^4 + 2\epsilon^2}}, \tag{11}$$

$$g_{\text{eff}}^{(\text{ord})} = -\frac{\left\langle [1 + 2\alpha\cos(2\pi x)]^4 \cos(q\pi x) \right\rangle}{1 + 2\alpha^2}, \tag{12}$$

with $\langle ... \rangle$ standing for the spatial average. Obviously, the effective nonlinearity coefficient given by expression (12) vanishes unless q takes values 0, 2, 4, 6, or 8. In particular, $g_{\text{eff}}^{(\text{ord})} = -(1 + 12\alpha^2 + 6\alpha^4)/(1 + 2\alpha^2)$ for $q = 0$, and $g_{\text{eff}}^{(\text{ord})} = -4\alpha(1 + 3\alpha^2)/(1 + 2\alpha^2)$ for $q = 2$. Actually, $g_{\text{eff}}^{(\text{ord})}$ does not vanish at $q = 2n$ with any integer n, if higher-order harmonics are kept in the expansion of the Bloch function at the edge of the semi-infinite gap, $1 + 2\sum_n \alpha_n\cos(2\pi n x)$, cf. the lowest-order approximation used in Eq. (9). With the value of the OL strength adopted in the numerical simulations reported above, $\epsilon = 5$, Eq. (11) yields $m_{\text{eff}}^{(\text{ord})} \approx 1.128$, which is virtually identical to the numerically found effective mass, see Eq. (??).

The soliton solution to Eq. (10) with an arbitrary amplitude, A, is

$$\Phi = A\exp\left(\frac{i}{2}g_{\text{eff}}^{(\text{ord})}A^2 t\right)\ \text{sech}\left(\sqrt{g_{\text{eff}}^{(\text{ord})}m_{\text{eff}}^{(\text{ord})}}Ax\right). \tag{13}$$

This solution explains scaling $W \propto 1/A$, which is observed in Fig. 2(b) for broad ordinary solitons in the case of $q = 2$. Figure 6 displays a direct comparison of profiles of a typical broad ordinary soliton, as obtained in the numerical form and produced by the averaging method. Good agreement between the two profiles is obvious [note that the figure displays the full wave function, $|\phi(x)|$, rather than the envelope, $\Phi(x)$, see Eq. (9)].

10

3.3 Gap solitons

3.3.1 Direct commensurability between the nonlinear and linear lattices

To apply the averaging approximation to GSs, which correspond to $g = -1$ in Eq. (1), we follow Ref. [30] and adopt the simplest ansatz which is relevant in this case,

$$\phi(x,t) = \Phi(x,t)\cos(\pi x),\tag{14}$$

with a slowly varying amplitude $\Phi(x,t)$. The difference in the form of the carrier wave in this expression, in comparison to Eq. (9), is due to the fact that, near the edge of the first finite bandgap, the Bloch function is close to a periodic function, whose period is twice as large as that of the underlying OL potential. On the contrary, near the edge of the semi-infinite gap the period of the Bloch function coincides with the OL's period.

The substitution of ansatz (14) in Eq. (1) and the application of the averaging method yields the respective asymptotic NLSE equation for the amplitude function,

$$i\frac{\partial\Phi}{\partial t} = -\frac{1}{2m_{\text{eff}}^{(\text{gap})}}\frac{\partial^2\Phi}{\partial x^2} + g_{\text{eff}}^{(\text{gap})}|\Phi|^2\Phi,\tag{15}$$

cf. Eq. (10). The effective mass and interaction coefficients in Eq. (15) are found to be

$$m_{\text{eff}}^{(\text{gap})} = \epsilon/\left(\epsilon - 2\pi^2\right),\tag{16}$$

$$g_{\text{eff}}^{(\text{gap})} = 2\left\langle(\cos(\pi x))^4\cos(q\pi x)\right\rangle.\tag{17}$$

Note that coefficient (17) is different from zero only for three values of q, *viz.*, $g_{\text{eff}}^{(\text{gap})}(q = 0) = 3/4$, $g_{\text{eff}}^{(\text{gap})}(q = 2) = 1/2$, and $g_{\text{eff}}^{(\text{gap})}(q = 4) = 1/8$. Together with

$$m_{\text{eff}}^{(\text{gap})} \approx -0.339,\tag{18}$$

which Eq. (16) yields for $\epsilon = 5$ (recall this value of the OL strength is fixed in the present work), the *complex conjugate* form of Eq. (15) gives rise to the usual soliton solutions for Φ^*, cf. solutions (13) for Φ. This fact gives the explanation to the scaling $W \propto 1/A$ for the broad GSs, as observed in Fig. 4(b) for $q = 2$. For stationary solutions, the complex conjugation implies, as mentioned above, the reversal of the sign of the chemical potential. This explains why the stability of the broad GSs obeys the "anti-VK" criterion, $d\mu/dN > 0$, which is simply the reverse of the ordinary negative-slope VK condition for the stable solutions of the equation for Φ^*.

The above description is also relevant for moving GSs. In particular, the comparison of the analytically predicted effective mass (18) to the empirical dynamical mass (**??**), drawn for the moving soliton from numerical data at $q = 2$, clearly demonstrates the high accuracy of the averaging approximation for the broad GSs, both static and moving ones.

3.3.2 Subharmonic commensurability between the nonlinear and linear lattices

The above approximation for GSs does not produce any definite result for $q = 1$, when the period of the NL in Eq. (1) is twice as large as OL's period (the subharmonic resonance between the nonlinear and linear lattices, as defined above). To derive an

effective envelope equation in this case, we notice that the substitution of original ansatz (14) in Eq. (1) and making use of the same effective mass as given by Eq. (16), but without averaging the nonlinear term, gives rise to the following equation:

$$i\frac{\partial \Phi}{\partial t} = -\frac{1}{2m_{\text{eff}}^{(\text{gap})}}\frac{\partial^2 \Phi}{\partial x^2} + \cos^3(\pi x)\,|\Phi|^2\Phi,\tag{19}$$

where it is taken into regard that $q = 1$. This equation suggests that ansatz (14) should be replaced by the following one, for stationary solutions:

$$\phi(x,t) = e^{-i\mu t}\left[\Phi_1(x)\cos(\pi x) + \Phi_4(x)\cos^4(\pi x)\right],\tag{20}$$

where both functions Φ_1 and Φ_4 are slowly varying ones. The substitution of ansatz (20) into Eq. (1) and straightforward trigonometric expansions make it possible to eliminate Φ_4 in favor of Φ_1:

$$\Phi_4(x) = \left(\mu - \frac{\pi^2}{2m_{\text{eff}}^{(\text{gap})}}\right)^{-1}|\Phi_1(x)|^2\,\Phi_1(x).\tag{21}$$

The remaining equation for $\Phi_1(x)$ is the NLSE with the *quintic* self-focusing nonlinear term:

$$\mu\Phi_1 = -\frac{1}{2m_{\text{eff}}^{(\text{gap})}}\frac{\partial^2 \Phi_1}{\partial x^2} - \frac{15m_{\text{eff}}^{(\text{gap})}}{8\left(\pi^2 - 2m_{\text{eff}}^{(\text{gap})}\mu\right)}|\Phi_1|^4\Phi_1.\tag{22}$$

An obvious soliton solution to Eq. (22) with arbitrary amplitude A is

$$\Phi_1 = A\,\sqrt{\text{sech}\,(kx)},\ k = \sqrt{5}m_{\text{eff}}^{(\text{gap})}\left(\pi^2 - 2m_{\text{eff}}^{(\text{gap})}\mu\right)^{-1/2}A^2,\ \mu = -\left(8m_{\text{eff}}^{(\text{gap})}\right)^{-1}k^2.\tag{23}$$

Solution (23) yields the scaling relation $W \propto 1/A^2$, which explains the same scaling that was observed, at $q = 1$, for broad GSs in Fig. 4(b).

It is necessary to mention that the nonstationary version of Eq. (22), with $\mu\Phi_1$ replaced by $i\partial\Phi_1/\partial t$, corresponds to the one-dimensional NLSE with the critical (quintic, in the 1D case) self-focusing nonlinearity, whose solutions, tantamount to those given by Eq. (23), are the so-called "one-dimensional Townes solitons". It is well known that the entire family of such solitons is unstable (see, e.g., Ref. [34]). Nevertheless, simulations of Eq. (1) demonstrate that the GSs approximated by the asymptotic solution (23) form a *stable* family, as long as the solitons remain broad, see the corresponding stable branch in Fig. 4(b). Thus, the asymptotic description of the broad GSs by means of Eq. (22) is valid, at $q = 1$, only for static solutions, while their dynamical behavior does not obey the straightforward time-dependent version of this equation.

4   Conclusion

We have investigated the existence, stability and mobility of ordinary solitons and GSs (gap solitons) in the 1D model combining nonlinear and linear periodic lattices in the Gross-Pitaevskii equation for the nearly one-dimensional BEC. The emphasis was made on the study of effects of the commensurability and incommensurability between the lattices, as well as on the development of analytical methods – the VA (variational approximation) for narrow ordinary solitons, and averaging method for broad solitons

of both types. We have demonstrated that, in the case of the direct commensurability between the lattices (equal periods), the ordinary solitons are similar to their counterparts in the free space. In the case of the subharmonic commensurability and incommensurability, the situation is different, featuring the existence threshold for the solitons, and a different scaling relation between their amplitude and width. Similar scaling relations are found for GS families, which demonstrate the bistability in cases different from the direct commensurability. Ordinary solitons may travel long distances, if kicked. Broad GSs are mobile too, although collisions between them are inelastic.

The analytical approximations demonstrate good accuracy in appropriate parameter regions. In particular, they correctly explain different scaling relations for the soliton families at different commensurability orders. As concerns the stability of the ordinary solitons, it is accurately predicted by the VK criterion. Simultaneously, the stability of GSs obeys the "anti-VK" criterion, an explanation to which was given by means of the effective equation produced through the averaging method. A notable feature of the present model is that it gives rise to characteristics $\mu(N)$ for the GSs that feature turning points (except for the case of the direct commensurability). Unlike previously studied models with the constant nonlinearity coefficient, the presence of the turning points has made it possible to test the anti-VK stability criterion for the GS families.

The analysis reported in this work may be naturally extended by studying GSs in higher finite bandgaps; in particular, a challenging issue is to verify the "anti-VK" stability criterion in the higher gaps. It may also be interesting to develop a systematic analysis of the commensurability for solitons and solitary vortices in the 2D model based on the combination of linear and nonlinear lattices.

References

[1] V. A. Brazhnyi and V. V. Konotop, Mod. Phys. Lett. B **18**, 627 (2004); O. Morsch and M. Oberthaler, Rev. Mod. Phys. **78**, 196 (2006).

[2] B. A. Malomed, D. Mihalache, F. Wise, and L. Torner, J. Optics B: Quant. Semicl. Opt. **7**, R53 (2005).

[3] B. A. Malomed, Z. H. Wang, P. L. Chu, and G. D. Peng, J. Opt. Soc. Am. B **16**, 1197 (1999).

[4] N. K. Efremidis, S. Sears, D. N. Christodoulides, J. W. Fleischer, and M. Segev, Phys. Rev. E **66**, 046602 (2002); J. W. Fleischer, T. Carmon, M. Segev, N. K. Efremidis, and D. N. Christodoulides, Phys. Rev. Lett. **90**, 023902 (2003); J. W. Fleischer, M. Segev, N. K. Efremidis, and D. N. Christodoulides, Nature **422**, 147 (2003); D. Neshev, E. A. Ostrovskaya, Y. Kivshar, and W. Królikowski, Opt. Lett. **28**, 710 (2003); D. N. Neshev, T. J. Alexander, E. A. Ostrovskaya, Y. S. Kivshar, H. Martin, I. Makasyuk, and Z. Chen, Phys. Rev. Lett. **92**, 123903 (2004); J. W. Fleischer, G. Bartal, O. Cohen, O. Manela, M. Segev, J. Hudock, and D. N. Christodoulides, *ibid.* **92**, 123904 (2004); Z. Chen, H. Martin, E. D. Eugenieva, J. Xu, and A Bezryadina, *ibid.* **92**, 143902 (2004); Z. Chen, M. Stepić, C. Rüter, D. Runde, D. Kip, V. Shandarov, O. Manela, and M. Segev, Opt. Express **13**, 4314 (2005); R. Fischer, D. Träger, D. N. Neshev, A. A. Sukhorukov, W. Królikowski, C. Denz, and Y. S. Kivshar, Phys. Rev. Lett. **96**, 023905 (2006).

[5] A. Szameit, D. Blömer, J. Burghoff, T. Schreiber, T. Pertsch, S. Nolte, and A. Tünnermann, Opt. Express **13**, 10552 (2005); D. Blömer, A. Szameit, F. Dreisow, T. Schreiber, S. Nolte, and A. Tünnermann, *ibid.* **14**, 2151 (2006); A. Szameit, J. Burghoff, T. Pertsch, S. Nolte, A. Tünnermann, and F. Lederer, *ibid* **14**, 6055 (2006).

[6] Y. V. Kartashov, V. A. Vysloukh, and L. Torner, Progress in Optics **52**, 63 (ed. by E. Wolf: North Holland, Amsterdam, 2009).

[7] F. Lederer, G. I. Stegeman, D. N. Christodoulides, G. Assanto, M. Segev, and Y. Silberberg, Phys. Rep. **463**, 1 (2008).

[8] W. A. Harrison, *Pseudopotentials in the Theory of Metals* (Benjamin, New York, 1966).

[9] T. Mayteevarunyoo, B. A. Malomed, and G. Dong, Phys. Rev. A **78**, 053601 (2008).

[10] H. Sakaguchi and B. A. Malomed, Phys. Rev. E **72**, 046610 (2005).

[11] F. K. Abdullaev and J. Garnier, Phys. Rev. A **72**, 061605(R) (2005); G. Theocharis, P. Schmelcher, P. G. Kevrekidis, and D. J. Frantzeskakis, *ibid.* A **72**, 033614 (2005); Y. Sivan, G. Fibich, and M. I. Weinstein, Phys. Rev. Lett. **97**, 193902 (2006); G. Fibich, Y. Sivan, and M. I. Weinstein, Physica D **217**, 31 (2006); J. Belmonte-Beitia, V. M. Pérez-García, V. Vekslerchik, and P. J. Torres, Phys. Rev. Lett. **98**, 064102 (2007); D. A. Zezyulin, G. L. Alfimov, V. V. Konotop, and V. M. Perez-Garcia, Phys. Rev. A **76**, 013621 (2007); P. Niarchou, G. Theocharis, P. G. Kevrekidis, P. Schmelcher, and D. J. Frantzeskakis, *ibid.* **76**, 023615 (2007); M. A. Porter, P. G. Kevrekidis, B. A. Malomed, and D. J. Frantzeskakis, Physica D **229**, 104 (2007); J. Zhou, C. Xue, Y. Qi, and S. Lou, Phys. Lett. A **372**, 4395 (2008); Y. V. Kartashov, V. A. Vysloukh, and L. Torner, Opt. Lett. **33**, 1747 (2008); A. S. Rodrigues, P. G. Kevrekidis, M. A. Porter, D. J. Frantzeskakis, P. Schmelcher, and A. R. Bishop, Phys. Rev. A **78**, 013611 (2008); J. Belmonte-Beitia, V. M. Pérez-García, V. Vekslerchik, and P. J. Torres, Discrete Contin. Dyn. Syst. B **9**, 221 (2008); F. Abdullaev, A. Abdumalikov, and R. Galimzyanov, Phys. Lett. A **367**, 149 (2009); V. M. Pérez-García R. Pardo, Physica D **238**, 1352 (2009); F. K. Abdullaev, R. M. Galimzyanov, M. Brtka, and L. Tomio, Phys. Rev. E **79**, 056220 (2009).

[12] C. H. Tsang, B. Malomed, and K. W. Chow, Discrete Contin. Dyn. Syst. S, in press.

[13] D. Witthaut, S. Mossmann, and H. J. Korsch, J. Phys. A: Math. Gen. **38**, 1777 (2005).

[14] B. A. Malomed and M. Ya. Azbel, Phys. Rev. B **47**, 10402 (1993).

[15] M. I. Rodas-Verde, H. Michinel, and V. M. Pérez-Garc ía, Phys. Rev. Lett. **95**, 153903 (2005); A. V. Carpentier, H. Michinel, M. I. Rodas-Verde, and V. M. Pérez-García, Phys. Rev. A **74**, 013619 (2006).

[16] J. Garnier and F. K. Abdullaev, Phys. Rev. A **74**, 013604 (2006).

[17] F. K. Abdullaev, A. Gammal, M. Salerno, and L. Tomio, Phys. Rev. A **77**, 023615 (2008).

[18] Y. V. Kartashov, B. A. Malomed, V. A. Vysloukh, and L. Torner, Opt. Lett. **34**, 3625 (2009).

[19] J. Belmonte-Beitia, V. M. Pérez-García, V. Vekslerchik, and V. V. Konotop, Phys. Rev. Lett. **100**, 164102 (2008).

[20] H. Sakaguchi and B. A. Malomed, Phys. Rev. E **72**, 046610 (2005); H. Sakaguchi and B. A. Malomed, Phys. Rev. A **75**, 063825 (2007); F. W. Ye, Y. V. Kartashov, B. Hu, and L. Torner, Opt. Exp. **17**, 11328 (2009); Y. V. Kartashov, B. A. Malomed, V. A. Vysloukh, and L. Torner, Opt. Lett. **34**, 770 (2009).

[21] L. Bergé, V. K. Mezentsev, J. Juul Rasmussen, P. L. Christiansen, and Yu. B. Gaididei, Opt. Lett. **25**, 1037 (2000); I. Towers and B. A. Malomed, J. Opt. Soc. Am. **19**, 537 (2002).

[22] R. Hao, R. Yang, L. Li, and G. Zhou, Opt. Commun. **281**, 1256 (2008); Y. V. Kartashov, V. A. Vysloukh, and L. Torner, Opt. Lett. **33**, 1774 (2008).

[23] Y. Kominis, Phys. Rev. E **73**, 066619 (2006); Y. Kominis and K. Hizanidis, Opt. Lett. **31**, 2888 (2006); Y. Kominis and K. Hizanidis, Opt. Express **16**, 12124 (2008).

[24] Y. V. Kartashov, V. A. Vysloukh, A. Szameit, F. Dreisow, M. Heinrich, S. Nolte, A. Tünnermann, T. Pertsch, and L. Torner, Opt. Lett. **33**, 1120 (2008).

[25] Z. Rapti, P. G. Kevrekidis, V. V. Konotop, and C. K. R. T. Jones, J. Phys. A: Math. Theor. **40**, 14151 (2007).

[26] J. Belmonte-Beitia, V. V. Konotop, V. M. Pérez-García. and V. E. Vekslerchik, Chaos, Solitons & Fractals **41**, 1158 (2009).

[27] Y. Sivan, G. Fibich, B. Ilan, and M. I. Weinstein, Phys. Rev. E **78**, 046602 (2008); Y. V. Kartashov, V. A. Vysloukh, and L. Torner, Opt. Lett. **33**, 2173 (2008); F. W. Ye, Y. V. Kartashov, B. Hu, and L. Torner, Opt. Exp. **17**, 11328 (2009).

[28] P. Xie, Z.-Q. Zhang, and X. Zhang, Phys. Rev. E **67**, 026607 (2003); A. Ferrando, M. Zacarés, P. Fernández de Córdoba, D. Binosi, and J. A. Monsoriu, Opt. Express **11**, 452 (2003); **12**, 817 (2004); J. R. Salgueiro, Y. S. Kivshar, D. E. Pelinovsky, V. Simon, and H. Michinel, Stud. Appl. Math. **115**, 157 (2005); T. Mayteevarunyoo and B. A. Malomed, J. Opt. Soc. Am. B **25**, 1854 (2008); J. R. Salgueiro and Y. S. Kivshar, Eur. Phys. J. Special Topics **173**, 281 (2009).

[29] M. Vakhitov and A. Kolokolov, Izvestiya VUZov Radiofizika **16**, 1020 (1973) [in Russian; English translation: Radiophys. Quantum. Electron. **16**, 783 (1973)]; L. Bergé, Phys. Rep. **303**, 259 (1998).

[30] H. Sakaguchi and B. A. Malomed, J. Phys. B: At. Mol. Opt. Phys. **37**, 1443 (2004).

[31] A. Gubeskys, B. A. Malomed, and I. M. Merhasin, Stud. Appl. Math. **115**, 255 (2005).

[32] P. J. Y. Louis, E. A. Ostrovskaya, C. M. Savage, and Y. S. Kivshar, Phys. Rev. A **67**, 013602 (2003).

[33] H. Sakaguchi and B. A. Malomed, Phys. Rev. E **74**, 026601 (2006).

[34] F. K. Abdullaev and M. Salerno, Phys. Rev. A **72**, 033617 (2005).